INTERFACE

royalsocietypublishing.org/journal/rsif

Research

Cite this article: Justyn NM, Heine KB, Hood WR, Peteya JA, Vanthournout B, Debruyn G, Shawkey MD, Weaver RJ, Hill GE. 2022 A combination of red structural and pigmentary coloration in the eyespot of a copepod. *J. R. Soc. Interface* **19**: 20220169. https://doi.org/10.1098/rsif.2022.0169

Received: 2 March 2022
Accepted: 26 April 2022

Subject Category:
Life Sciences–Physics interface

Subject Areas:
evolution, biophysics, biochemistry

Keywords:
astaxanthin, carotenoids, Raman spectroscopy, structuralcolour, *Tigriopus californicus*, transmission electron microscopy

Authors for correspondence:
Nicholas M. Justyn
e-mail: nmj0005@auburn.edu
Kyle B. Heine
e-mail: kbh0039@auburn.edu

†Contributed equally to the study.

Electronic supplementary material is available online at https://doi.org/10.6084/m9.figshare.c.5978511.

THE ROYAL SOCIETY PUBLISHING

A combination of red structural and pigmentary coloration in the eyespot of a copepod

Nicholas M. Justyn[1,†], Kyle B. Heine[1,†], Wendy R. Hood[1], Jennifer A. Peteya[2], Bram Vanthournout[3], Gerben Debruyn[3], Matthew D. Shawkey[3], Ryan J. Weaver[4] and Geoffrey E. Hill[1]

[1]Department of Biological Sciences, Auburn University, Auburn, AL 36849, USA
[2]Department of Biology and Integrated Bioscience Program, The University of Akron, Akron, OH 44325, USA
[3]Department of Biology, Evolution and Optics of Nanostructures Group, University of Ghent, Ghent, Belgium
[4]Department of Ecology, Evolution, and Organismal Biology, Iowa State University, Ames, IA 50011, USA

NMJ, 0000-0002-6561-9889; KBH, 0000-0002-0557-4551; WRH, 0000-0002-8398-3908; JAP, 0000-0001-6218-2637; BV, 0000-0001-6198-9092; MDS, 0000-0002-5131-8209; RJW, 0000-0002-6160-4735; GEH, 0000-0001-8864-6495

While the specific mechanisms of colour production in biological systems are diverse, the mechanics of colour production are straightforward and universal. Colour is produced through the selective absorption of light by pigments, the scattering of light by nanostructures or a combination of both. When *Tigriopus californicus* copepods were fed a carotenoid-limited diet of yeast, their orange-red body coloration became faint, but their eyespots remained unexpectedly bright red. Raman spectroscopy indicated a clear signature of the red carotenoid pigment astaxanthin in eyespots; however, refractive index matching experiments showed that eyespot colour disappeared when placed in ethyl cinnamate, suggesting a structural origin for the red coloration. We used transmission electron microscopy to identify consecutive nanolayers of spherical air pockets that, when modelled as a single thin film layer, possess the correct periodicity to coherently scatter red light. We then performed microspectrophotometry to quantify eyespot coloration and confirmed a distinct colour difference between the eyespot and the body. The observed spectral reflectance from the eyespot matched the reflectance predicted from our models when considering the additional absorption by astaxanthin. Together, this evidence suggests the persistence of red eyespots in copepods is the result of a combination of structural and pigmentary coloration.

1. Introduction

Animal coloration is produced by the absorption of light by pigments, the scattering of light by a structure, or a combination of the two mechanisms [1]. Pigmentary and structural coloration are distinct in their ontogeny and mechanisms of colour production, but disentangling the relative importance of microstructures versus pigments in the production of a specific colour display can be challenging [2,3]. Such is the case with the brilliant red eyespot coloration of copepods, which has drawn the attention of biologists since the nineteenth century [4]. Precursor/product feeding experiments documented that *Tigriopus californicus* copepods use a variety of dietary carotenoids to synthesize astaxanthin, and the high concentrations of free and esterified astaxanthin were implicated as the source of orange-red body coloration. In previous studies, when *T. californicus* copepods were fed a carotenoid-restricted diet, their bodies became nearly clear [5]. This observation is consistent with the hypothesis that orange-red coloration is a product of carotenoid pigments because, like most animals, copepods are not known to synthesize carotenoids *de novo*. Rather, copepods ingest carotenoids as intact pigments that are then

incorporated into their bodies [6]. Once carotenoids are ingested, they can be either deposited directly or bioconverted into new carotenoids [7]. However, even as the bodies of copepods that are deprived of carotenoids faded to be nearly colourless, their eyespots remain a vivid red colour [5,8]. Thus, while carotenoids were shown to play an important role in the coloration of copepods, further observations implicate additional mechanisms in the production of red eyespot coloration in copepods.

One explanation for the origin of eyespot coloration is that copepods might endogenously produce other red pigments such as ommochromes [9,10]. Alternatively, the seemingly non-iridescent red colour of the eyespot could be produced by nanostructures that coherently scatter red light. There are many examples of structural colour in arthropods [11–15] and even in some species of copepods [16,17]. In each of these cases, coloration is produced by fixed structures with high refractive index contrast, typically chitin and air, that possess the correct periodicity to coherently scatter light in the visible spectrum [18,19]. However, non-iridescent red structural colour is rarely observed in nature, but iridescent red structural colour is common and is sometimes combined with pigments, which reduces the iridescent appearance [20–22].

Here, we investigated the mechanisms responsible for the red coloration of the eyespots of *T. californicus* copepods to better understand how colour is being maintained in the absence of carotenoids. We first used Raman spectroscopy to detect pigments in the eyespots, and refractive index matching experiments to test for structural coloration in eyespots. We performed transmission electron microscopy (TEM) to visualize and measure any structures capable of producing colour. We then modelled the predicted reflectance produced by the nanolayers found within the exoskeleton and used microspectrophotometry to verify our model predictions.

Based on our observations in these procedures, we conclude that *T. californicus* copepods create their red eyespot coloration using a combination of structural colour, produced by consecutive nanolayers of spherical air pockets in the exoskeleton, and pigmentary colour, by retaining small amounts of astaxanthin. The nanostructures within the exoskeleton effectively act as a single thin film because there is little exoskeleton between each layer, and individually each layer is too small to coherently scatter light in the visible spectrum. Astaxanthin reduces the iridescence of this thin film and enhances the red coloration of the eyespot. Our findings not only provide evidence of a novel colour production mechanism in arthropods but also demonstrate a means to circumvent the apparent biological difficulty of producing brilliant non-iridescent, red coloration using nanostructures. This is accomplished by combining iridescent, red structural coloration with orange-red pigments.

2. Material and methods

We took a systematic approach to identify colour production mechanisms throughout the body of *T. californicus* copepods. We began by performing light microscopy to determine which regions of the body expressed visible colour and which regions were most suitable to evaluate the mechanisms of colour production, while avoiding undigested algae in the digestive tract. We then performed Raman spectroscopy on the body and eyespot, and then compared those signals to Raman spectra obtained from carotenoid standards. We chose confocal Raman spectroscopy rather than traditional HPLC because Raman requires a minimal amount of tissue to analyse and can be localized to exceedingly small areas of the body, such as an individual eyespot on a copepod. Next, we used refractive index matching experiments to detect if structural coloration was present, and once confirmed, we used TEM to identify and measure the spacing of any nanostructures that are present. We then modelled the predicted reflectance of the structures using the transfer matrix method [23]. Lastly, we measured the reflectance of the body and eyespot of the copepods using microspectrophotometry and compared it to the reflectance predicted by our models.

2.1. Copepod husbandry

We collected *Tigriopus californicus* copepods near San Diego, CA, USA in 2014 and cultured them in our laboratory at 20–22°C, salinity = 32 psu. Copepods were fed ad libitum *Isochrysis galbana* and *Tetraselmis chuii* algae on a natural light cycle, which provide the required precursor carotenoids for red coloration [5]. Carotenoid-restricted copepods were fed ad libitum Bragg Nutritional Yeast, which lacks the carotenoids responsible for producing orange-red coloration throughout the body [5]. Yeast-fed individuals were raised in the dark and were approximately four months, or four generations, removed from the algae-fed, red-coloured population.

2.2. Colour investigation (light microscopy and refractive index matching)

Copepods were photographed on a glass slide using an AmScope microscope digital camera at 1× and 4× magnifications to capture the appearance of the body and eyespot. Five copepods from both treatment groups were then dissected in half using a hypodermic needle, and a drop of ethyl cinnamate, acetone, water, or nothing was placed on each individual in a covered Petri dish ($n = 10$). Pictures were taken after 5 min and 24 h. Ethyl cinnamate, with a refractive index of 1.558 [24], was chosen because it approximates the relatively high refractive index of the exoskeleton. Ethyl cinnamate has previously been shown to produce detectable changes in the structural colour of spider cuticles that have a refractive index of approximately 1.60 [25].

2.3. Pigment identification (Raman spectroscopy)

We characterized the carotenoids present in *T. californicus* eyespots and bodies using confocal Raman spectroscopy. Raman spectroscopy is a technique that has been previously employed to characterize carotenoids present in different animal tissues, including spider silk and bird feathers [3,21,26]. After allowing copepods to visibly air dry, we analysed whole specimens, including two male and two female algae-fed copepods, as well as two male and three female yeast-fed copepods. To assess changes in carotenoid composition under diet restriction, both algae- and yeast-fed copepods were sampled in the same anatomic positions, including two eyespot locations, the cephalosome, metasome, urosome and one caudal ramus (figure 1). We found that the eyespots were completely covered by the exoskeleton. So, to avoid analysing the exoskeleton rather than the underlying eyespots, we removed the eyespots from one algae- and one yeast-fed copepod using a pin sterilized in 200 proof ethanol. We then bisected the eyespots to expose the centre. All copepod samples were attached to a glass slide using clear, double-sided tape. We compared Raman spectra from copepod samples to those of an astaxanthin reference standard (DSM, Heerlen, Netherlands).

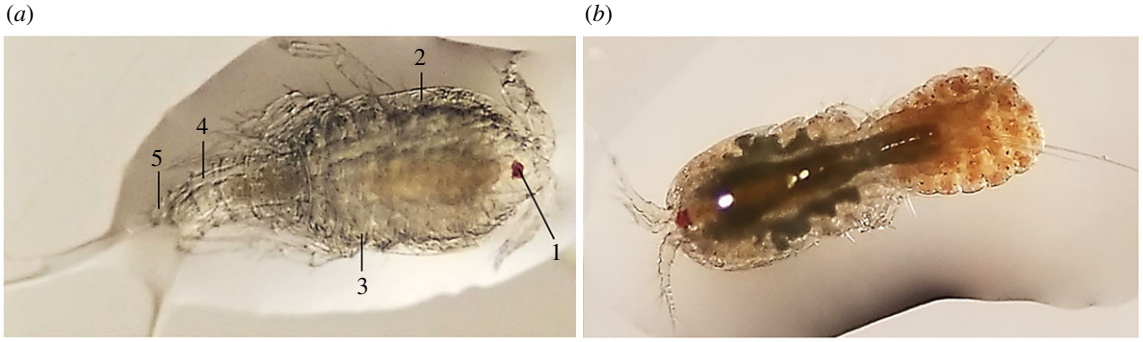

Figure 1. Light microscopy indicating Raman sampling locations of both yeast- and algae-fed *Tigriopus californicus* copepods. (*a*) Male fed a carotenoid-restricted diet of yeast, including the (1) eyespot, (2) cephalosome, (3) metasome, (4) urosome and (5) caudal ramus. (*b*) Red, algae-fed female with an egg sac. Both copepods are approximately 1–2 mm in size.

We captured Raman spectra using a 532 nm excitation laser through a 50× objective with a numerical aperture of 0.75 and a working distance of 0.37 mm on a LabRam high resolution Raman microscope (HORIBA Scientific), calibrated with a wafer of pure silicon, at the Surface and Optical Analysis (SOA) Facility at The University of Akron. We used a 100 µm slit aperture, a 400 µm pinhole, an integration time of 5 s × 1 accumulation, and a grating of 1200 lines per mm. We collected spectra from at least two different locations on each copepod eye sample and four different body regions on each whole copepod sample. When analysing whole copepod samples, we specifically sampled four body regions near the periphery of the animal to avoid the alimentary canal, which appears darkly coloured in all samples, and any undigested food within it. Pigmented copepods and eyespot samples were analysed using a D2 (1%) filter, while clear samples were analysed using a D1 (10%) filter to decrease fluorescence and sharpen the Raman peaks, making them more comparable to those of the red copepod samples. To account for any potential influence from the adhesive, we also took Raman spectra from the double-sided tape using both D1 and D2 filters. Cosmic ray spikes were removed from the spectra, and each sample was checked for burning after each spectrum was collected. No samples were burned. We normalized all of the spectra using Origin Pro v. 8.5.1 (OriginLab), then used IgorPro v. 6.36 (Wavemetrics) to fit the Raman peaks using a Gaussian distribution and a linear baseline.

2.4. Structural characterization and quantification (TEM measurements)

We prepared all copepods for TEM following previously established methods [27]. First, we placed the copepods into a primary fixative consisting of 12.5 ml of 0.2 M phosphate buffer, 6.25 ml of 10% glutaraldehyde, 5 ml of 10% formaldehyde and 1.25 ml of dH_2O. We then removed the distal portion of the urosome and placed the remaining portion of the copepod into primary fixative overnight at 4°C to allow the fixative to thoroughly infiltrate the copepod. Next, we washed the sample three times in 0.1 M phosphate buffer for 30 min each time before placing it into a secondary fixative of 2% osmium tetroxide in the dark for 90 min. We then dehydrated the samples using a seven-step dehydration series and placed the samples into the transitional fluid propylene oxide (PO). We then infiltrated the tissue with a PO:Epon resin ratio of 2 : 1, 1 : 1, 1 : 2, and pure Epon resin over 12 days, for three days per ratio [28]. Samples were cured at 70°C for 24 h. Each copepod was embedded longitudinally to consistently section the eyespots. We cut ultrathin, 80 nm thin cross sections and collected them on 200 mesh copper grids. We stained each of the sections with uranyl acetate and lead citrate to increase contrast. We completed TEM using a ZEISS EM10 transmission electron microscope in the Auburn University Research Instrumentation Facility.

We measured the thickness of the epicuticle, exocuticle, individual spherical nanostructure layers, and the total thickness of all layers combined, in each of the representative TEM images. Measurements were made at ten random locations and averaged to obtain representative measurements for each of the aforementioned regions. We completed all measurements using ImageJ v. 1.53f [29].

2.5. Predicted and measured reflectance (thin-film optical modelling and microspectrophotometry)

The predicted peak reflectance of 300–700 nm from the structures was calculated using the transfer matrix method [23]. We used $n = 1$ for the refractive index of air and $n = 2$ for the darker pigmented sclerotin that comprises the epicuticle and exocuticle [14]. The thickness of the single air layer input into the model was adjusted depending on the number of individual spherical nanostructure layers found throughout different regions of the exoskeleton. We also ran the model using various other conditions to account for the possibility of a lower refractive index for chitin, closer to 1.56 [19,30], and other alternative conditions that could exist (see electronic supplementary material).

Using normal specular reflection microspectrophotometry, we measured the reflectance from the eyespot and body of six copepods. We used an AX10 UV–visible microspectrophotometer (CRAIC Technologies Inc.) to collect the reflectance spectra for each region using a 15× objective (10×10 µm^2 area) with black and white standards (Avantes WS-2 and BS-2), following the methods of Hsiung *et al*. [25]. As the images of the 15× objective are of lower quality, we present the images of the 10× objective in the Results section. The results were visualized using the pavo package in R [31,32]. Three measurements were obtained from each eyespot and body region of all six copepods. The three measurements from each region of each individual copepod were averaged to create the displayed spectra and shaded variance. The last row of microspec values were adjusted from 699.88 nm to 700 nm to prevent a conflict with calculations made in pavo.

3. Results

3.1. Colour investigation (light microscopy and refractive index matching)

Light microscopy revealed the extent of colour differences between the copepods raised on an algae diet versus those reared on a carotenoid-restricted, yeast diet (figure 1). The yeast-fed copepods lacked all but a trace of orange-red coloration throughout their body. However, these yeast-fed copepods retained their bright red eyespots, which appeared non-iridescent under both reflected and transmitted light.

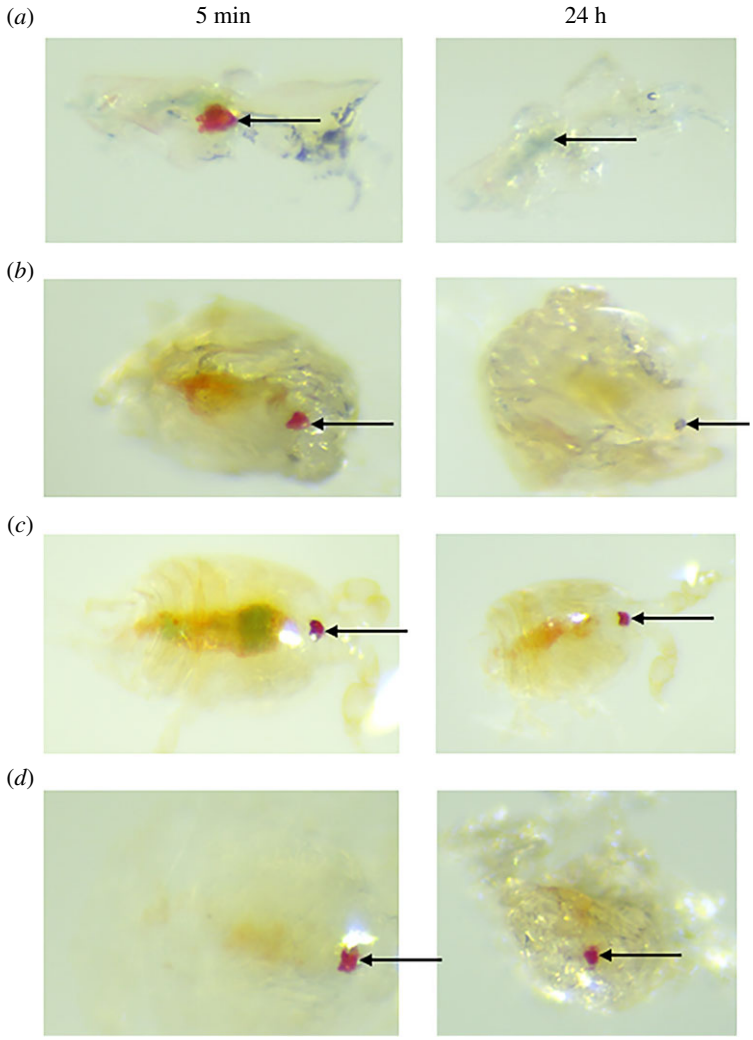

Figure 2. Refractive index contrast images. Refractive index matching under reflected light of copepods in (*a*) ethyl cinnamate where the eyespot coloration completely disappears, (*b*) acetone where the eyespot coloration is slightly faded, (*c*) water where the eyespot colour is consistent and (*d*) air where the eyespot colour is consistent after 24 h. Arrow indicates the eyespot location.

Refractive index matching experiments revealed that the copepods completely lost their eyespot colour when they were submerged in ethyl cinnamate, while they retained some portion of their colour when left in air, water, or acetone for 24 h (figure 2). The loss of colour in ethyl cinnamate is a result of the removal of refractive index contrast that is necessary for producing the structural colour. When the structures are filled with ethyl cinnamate, which has a similar refractive index to the exoskeleton, the structural colour disappears (figure 2*a*). Ethyl cinnamate is a highly viscous liquid, so we allowed an extended period of time to allow the ethyl cinnamate to penetrate structures. The orange-red colour of the copepod throughout the body persisted in the samples submerged in ethyl cinnamate, indicating that the removal of the red eyespot coloration was not simply the result of carotenoid extraction (figure 2*a*). By contrast, the orange-red colour faded from the body of copepods when submerged in acetone, which is a carotenoid solvent (figure 2*b*). The eyespot colour was also diminished in an acetone solution, indicating that a portion of eyespot coloration was due to carotenoid pigments (figure 2*b*).

3.2. Pigment identification (Raman spectroscopy)

Raman spectra for all samples, including the copepod eyespots of both algae- and yeast-fed copepods, body and carotenoid standards, had three main peaks: one between 1005 cm^{-1} and 1008 cm^{-1}, a second peak between 1151 cm^{-1} and 1159 cm^{-1} and a third peak between 1507 cm^{-1} and 1525 cm^{-1} (figure 3). These three intense peaks are diagnostic of the presence of a carotenoid pigment in the sample [26,33]. Previously reported Raman spectra for chitin lack similar peaks [34], suggesting that despite our attempts to deprive the yeast-fed copepods of dietary carotenoids—and the clear, colourless appearance of their cuticles—they still deposited detectable amounts of carotenoids in their bodies and eyespots.

The region between the second and third major carotenoid peaks, referred to as the 'fingerprint region' [35], can be used to identify specific carotenoids. The fingerprint region for the red eyespots in both algae- and yeast-fed copepods matched each other, and that of the astaxanthin standard (figure 3). An identical signature was identified for the body (i.e. cephalosome, metasoma and urosome) of both female and male, red-coloured individuals.

3.3. Structure characterization and quantification (TEM measurements)

Using TEM and measurements made in ImageJ, we determined the epicuticle was 35.1 nm ± 8.6 nm ($n = 50$ from five images and two copepods) and the exocuticle to be

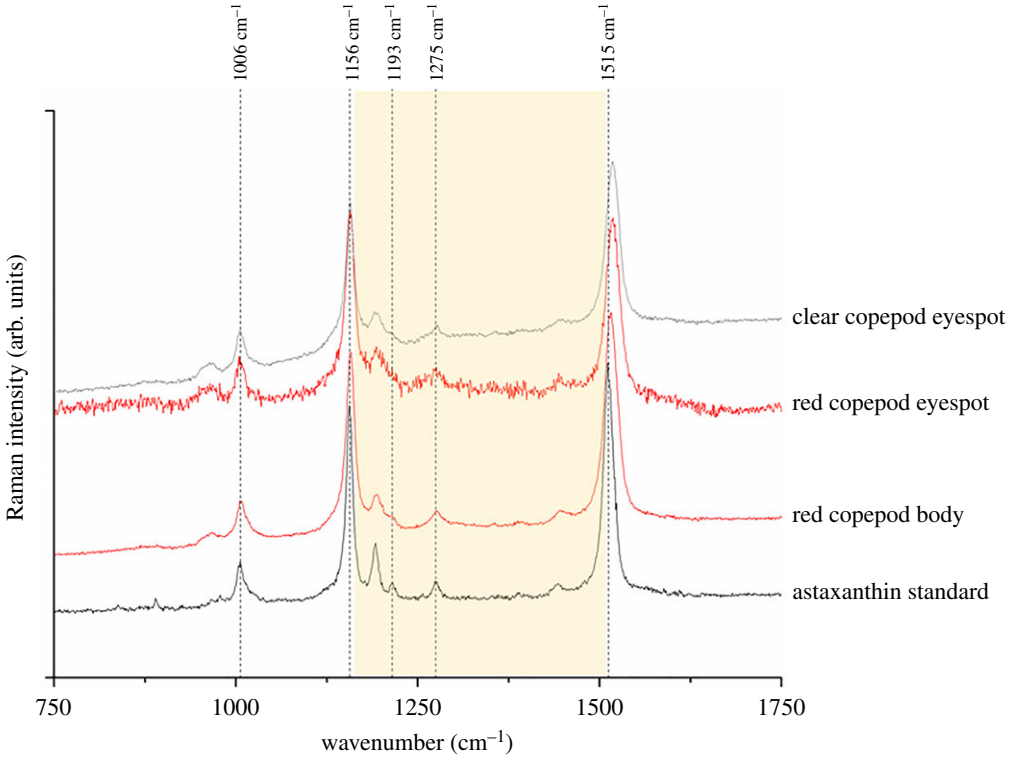

Figure 3. Raman spectra for copepods and carotenoid standards including proposed astaxanthin peaks. The black spectra indicate standards, red indicates spectra from red (algae-fed) copepods, and grey indicates spectra from clearer (yeast-fed) copepods. The yellow highlighted region indicates the fingerprint region. 'Body' corresponds to sampling locations 2–5 in figure 1.

536.4 nm ± 135.5 nm thick ($n = 50$ from five images and two copepods). TEM also revealed distinct nanolayers between the epicuticle and exocuticle of the exoskeleton (figure 4). Their shape and low electron density suggested that these structures are likely air spaces. The number of air layers varies throughout the exoskeleton of a copepod, and multiple air layers are seen even when examining ultrathin sections from the eyespot region of the copepod. With an average spacing of 34.6 nm ± 4.6 nm ($n = 50$ from five images and two copepods), the individual air layers appear too small to produce structural colour by acting as a true multilayer of alternating chitin and air. However, if the width of multiple air layers combined is considered, the layers could act as a single thin film, with the correct periodicity and refractive index contrast to coherently scatter visible light. A similar phenomenon occurs in feathers where some melanosomes are placed so close together in the barbules that they act as a single layer [10,22,36,37]. We observed variation in the number of air layers found depending on which region of the copepod was sampled. When the area of the exoskeleton above the eyespot region was sampled, three to four air layers were encountered. Throughout the body, variation between one and two air layers was most frequently encountered. The measurements for the thickness of multiple air layers included the thickness of the air layers as well as the small amount of exocuticle between them. We determined the width of two air layers to be 81.5 nm ± 6.4 nm ($n = 10$ from one image and one copepod), 168.2 nm ± 17.3 nm for three air layers ($n = 40$ across four images and one copepod), and 220.5 nm ± 33.0 nm for four air layers ($n = 30$ across three images and one copepod; see electronic supplementary material, figure S1).

3.4. Predicted and measured reflectance (thin-film optical modelling and microspectrophotometry)

Using the transfer matrix method previously developed by Eliason *et al.* [23], we calculated the predicted peak reflectance between 300 and 700 nm [23]. We used the measurements obtained from our TEM images for the thickness of each layer and used previously reported values for the refractive index of air and sclerotized chitin in the model. We estimated the predicted reflectance of an exoskeleton with a single air layer using a refractive index of $n = 2$ for the epicuticle, $n = 1$ for one layer of air, and $n = 2$ for the exocuticle, an air layer thickness of 34.6 nm and an exoskeleton thickness of 536.4 nm. This resulted in a low amount of reflectance without a peak in the visible wavelengths of light, and some reflectance in the ultraviolet wavelengths of light (figure 5*a*). We used these same parameters, only varying the thickness of the air layer, to determine the predicted reflectance for each number of air layers observed in the exoskeleton. When two air layers are combined, with a thickness of 81.5 nm, they are predicted to produce a discrete peak at 326 nm in the UV-A range, and an overall higher amount of reflectance than one layer (figure 5*b*). Three air layers combined have an average thickness of 168.2 nm, and four air layers combined have an average thickness of 220.5 nm. Both three and four air layers present in the exoskeleton are predicted to maximally reflect long wavelengths of light in the orange-red region of the visible spectrum (figure 5*c*,*d*). In each figure, we also shaded the typical range (400–550 nm) that astaxanthin absorbs light, which peaks around 476–481 nm [38,39]. Since astaxanthin is co-deposited throughout the copepod body and eyespot, it should absorb a significant amount of the light in this region of the

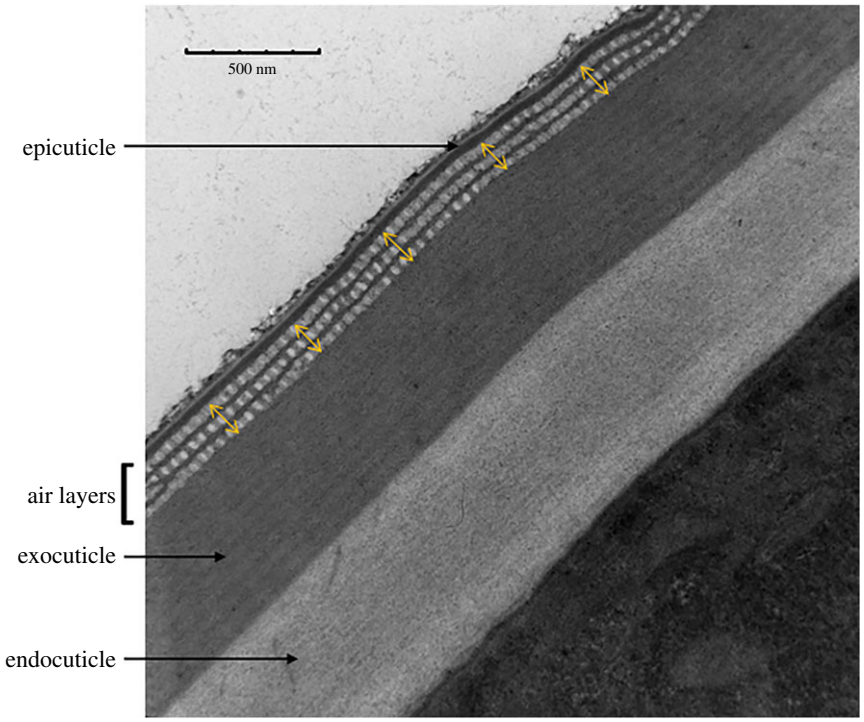

Figure 4. Transmission electron micrograph of nanolayers of air spheres found in the exoskeleton of *Tigriopus californicus* copepods. Yellow arrows correspond to random sampling locations. Scale bar = 500 nm.

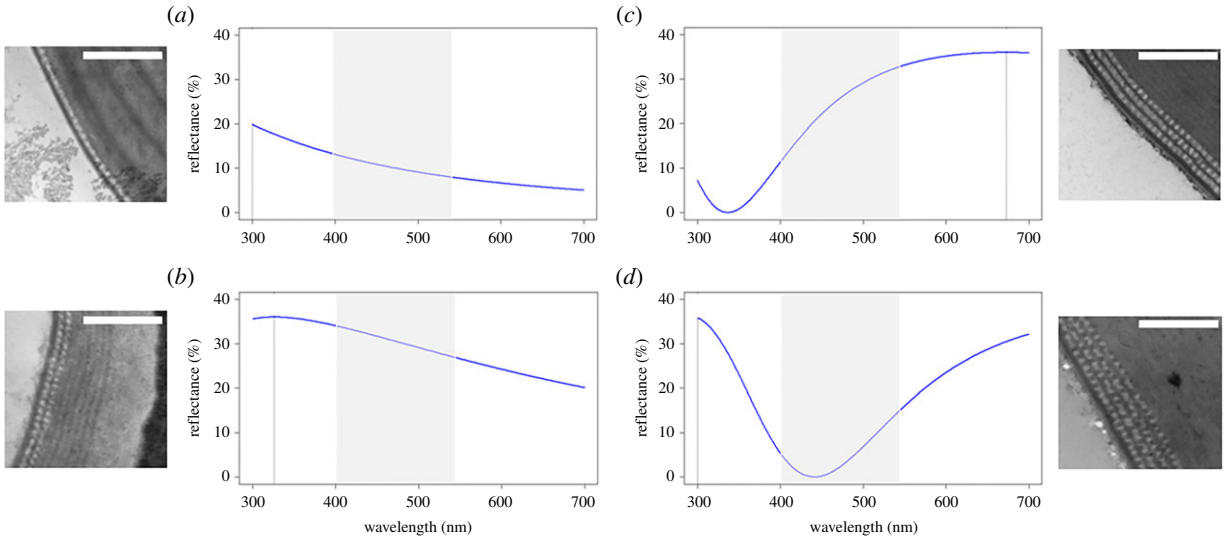

Figure 5. Periodicity of nanolayers of air spheres in the exoskeleton and predicted structural colour peak reflectance. (*a*) One air layer found throughout the body, (*b*) two air layers found throughout the body, (*c*) three air layers found in the eyespot region and (*d*) four air layers found in the eyespot region. The shaded region from 400 to 550 nm represents the typical absorption range for carotenoids. Scale bars = 500 nm.

visible spectrum. Although rare, we saw more than four layers of air spaces in small regions throughout the copepod exoskeleton. We estimated the thickness of any additional layer by increasing the thickness by 80 nm for each additional layer past four layers. These estimates from five to eight layers varied in the amount of reflectance produced, but seven and eight layers, with a spacing of 460 nm and 540 nm respectively, notably also produced a high amount of reflectance in the orange-red region of the visible spectrum (see electronic supplementary material, figure S2).

In addition to these calculations, we also changed each value in the model to alternative values to determine how, if at all, the predicted peak reflectance is impacted. While we chose to use an estimate of 2.0 for the refractive index of chitin based on previous work, changing the refractive index of chitin to a more conservative estimate of 1.56 does not change the hue of the predicted reflectance; however, it does lower the brightness by approximately half (see electronic supplementary material, figure S3). These refractive indices used encompass the range of values potentially attributed to sclerotized chitin. While the TEM images suggest that the spaces we observe are air layers, it is also possible that they are filled with water. To simulate this, we changed the refractive index of the air layers to 1.333 for water and ran additional models. This again significantly reduces the refractive index contrast between layers, and therefore decreases the brightness, while the hue once again remains unchanged (see electronic supplementary material, figure S4). Actual

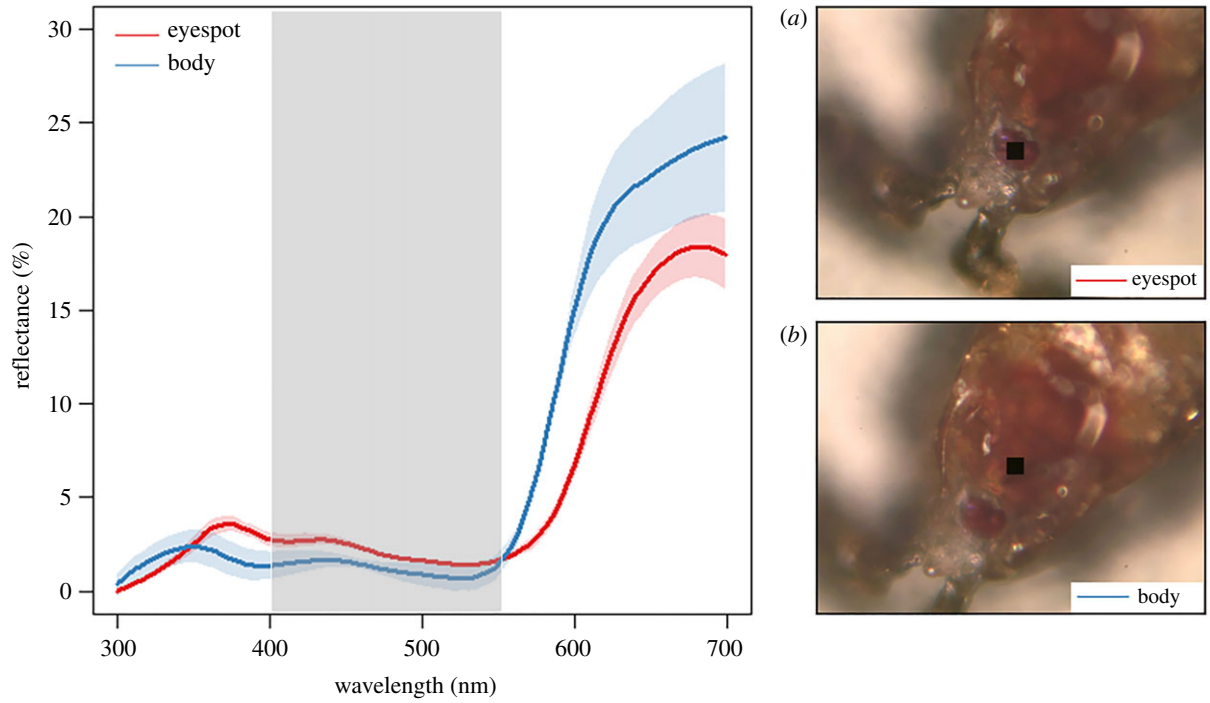

Figure 6. Reflectance spectra of astaxanthin and structural colour combined, measured using microspectrophotometry (15× objective) from a copepod eyespot (bottom red line) and body (top blue line). Three measurements from each region were averaged to create the displayed spectra and shaded variance. The grey shaded region from 400 to 550 nm represents the typical absorption range for carotenoids. Representative images of the (*a*) eyespot and (*b*) body were taken during microspectrophotometry using the 10× objective. The black square in each image represents the sampling location of the microspectrophotometer. See electronic supplementary material, figure S5, for the microspectrophotometry of all six individual copepod eyespots and bodies.

reflectance spectra obtained by microspectrophotometry mostly matched the reflectance spectra predicted by our models with three or four air layers (figure 5*c*,*d*; see electronic supplementary material, figure S5). However, reflectance in UV wavelengths was lower than predicted if four air layers are present, and the reflection of visible wavelengths began to increase at approximately 550, rather than approximately 500 nm (figure 5*d*). Both of these differences are likely due to the absorption of astaxanthin present in the eyespot. This also suggests that three or four air layers are most common above the eyespot, since the predicted reflectance of three and four layers most closely matches the observed reflectance. Importantly, these data confirmed the distinct colour difference between the red eyespot and the orange body (figure 6; electronic supplementary material, figure S4): reflectance in the body began to rise at shorter wavelengths than in the eyespot, presumably due to spherical, air-filled nanostructures above the eyespot.

4. Discussion

When *Tigriopus californicus* copepods are maintained through multiple generations on a yeast diet that provides limited access to carotenoids, their bodies lose almost all orange-red coloration. However, the eyespots of these same yeast-fed copepods remain bright red. To investigate the source of this red eyespot coloration, we employed a combination of chemical and microscopy techniques, which revealed that the red eyespot coloration is the result of a combination of astaxanthin and structural coloration.

Using Raman spectroscopy, we found that copepods on a carotenoid-restricted diet continue to incorporate astaxanthin into their eyespots. The source of the carotenoids used by these animals is unclear, but sufficient carotenoids must remain in their environment to maintain red eyespots even as red body coloration fades. Saturating a copepod section in ethyl cinnamate resulted in the loss of all red eyespot coloration. On the other hand, when we removed carotenoid pigments with the solvent acetone, a brown-red eyespot remained. The opposite was true for the orange body, which remained orange in ethyl cinnamate (figure 2*a*), but became transparent in acetone (figure 2*b*). This transition in eyespot coloration from scarlet to a more reddish brown is likely caused by the loss of light absorption in the middle of the visible spectrum by astaxanthin. By contrast, the body (i.e. not surrounding the eyespot) likely relies solely on pigments for coloration, so it becomes transparent following carotenoid removal via acetone. Additionally, a violet or purple colour is noticeable around the edge of the eyespot in the higher magnification images included in figure 6*a*,*b*. This further suggests a structural origin for the eyespot colour and matches our predicted reflectance for four layers of nanostructures (figure 5*d*).

To further investigate the hypothesis that nanostructures are involved in the red colour production of copepods, we studied the nanoscale components of sectioned copepods using TEM. These images revealed stacked nanolayers comprised of spherical pockets (which appear to be filled with air) in the exoskeleton throughout the body and above the eyespot region of the copepod. We repeatedly observed a pattern of three or four layers stacked together above the eyespots of copepods, and the total thickness of these stacked layers was 168.2 nm and 220.5 nm, respectively. The individual spherical nanostructures comprising the air layers appear to be relatively spherical in cross-sectional micrographs, suggesting that anisotropy in the form of elongated air spaces is not present. This is significant because it suggests that the structure is unlikely to interact with polarized light

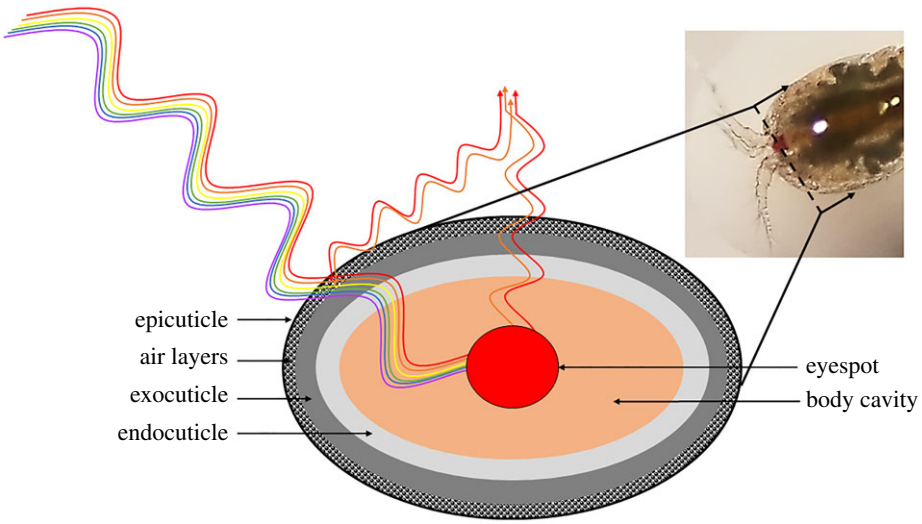

Figure 7. Proposed cross-section schematic for how light interacts with nanolayers of spheres deposited in the exoskeleton and astaxanthin deposited within the eyespot. Incident light first is coherently scattered by the three or four nanolayers of air spheres, and light is absorbed by the darker sclerotized exocuticle. Finally, any remaining light is absorbed by astaxanthin in the eyespot, and remaining orange-red wavelengths of light are reflected. The darker red colour of the eyespot is likely due to the presence of three or four layers of spheres deposited in the exoskeleton surrounding the eyespot which reflects orange-red light, as opposed to the one or two layers found in the exoskeleton throughout the rest of the body which reflects small amounts of UV light. Astaxanthin is deposited in the eyespot.

in a transformative way [40]. If these are not spheres, for instance if they are continuous tubes, we would expect some amount of variation in the cross sections, which we did not observe. The presence of one or two air layers throughout the exoskeleton could be advantageous to copepods by reflecting UV light and aiding in protection against UV radiation that is known to significantly influence survival and reproductive success in copepods that live in shallow splash pool habitats [41–43]. Carotenoids in both the body and eyespot additionally contribute to UV light absorption and, thereby, aid in UV protection.

Using the measurements obtained from TEM, we used the transfer matrix method to demonstrate that, when combined together, three and four layers of nanostructures possess the correct periodicity to coherently scattering orange-red light (590–700 nm). Microspectrophotometry from individual copepod eyespots confirmed high reflectance in these wavelengths, but with a somewhat later onset of increased reflectance (approx. 550 rather than the predicted 500 nm), and reduced UV reflectance compared to the model with four air layers, which are both likely caused by absorption of astaxanthin (figure 5*c*,*d*; see also figure 1) [44,45]. Microspectrophotometry also revealed similar levels of UV reflectance from both the eyespot and body regions of the copepods sampled; however, the location of the peak in the UV varied slightly, which is likely due to the presence of the nanostructures as well.

Taken together, these observations suggest that structural elements produce a base colour that is modified by astaxanthin via absorption of light in the middle of the visible light spectrum and UV. The presence of astaxanthin results in the redder hue, increased saturation, and reduced iridescence and UV reflectance of the eyespot coloration (figure 7). A combination of red structural colour and pigmentary colour is rare in animals, but the idea has been hypothesized previously. For instance, jumping spiders (*Maratus volans*) also combine red-orange ommochromes and red structural colour to create a non-iridescent, saturated, bright red colour [21]. We hypothesize that copepods combine both astaxanthin and structures in a similar manner to jumping spiders, which is why their eyespots appear non-iridescent under light microscopy. Jumping spiders and other bright red animals like house finches (*Haemorhous mexicanus*) produce red colour for display, but the red eyespot of a copepod is unlikely involved in sexual signalling [21,46,47]. Instead, the bright red eyespot colour, that is present in many other organisms as well, may have a functional role. Given the apparent maintenance of astaxanthin in the eyespot of *T. californicus*, we suspect there is a need to maintain red coloration in the eyespot. Unlike the more complex eyes of some other arthropods, the eyespots of copepods likely do not form cohesive images; rather, copepod eyespots detect changes in light versus dark and polarized light [48–54]. Because *T. californicus* resides primarily in shallow rock pools and cannot migrate to avoid UV light, the maintenance of astaxanthin in the eyespots may also play a protective role against UV light, similar to that in more complex eyes [55]. Carotenoids responsible for protection and light absorption are located in the retina of some animal eyes and are known for absorbing blue light and protecting photoreceptive cells, as well as quenching reactive oxygen species [56–58]. Alternatively, red coloration may allow individuals to preferentially absorb blue wavelengths of light more efficiently at night and during crepuscular hours in shallow waters. As such, we speculate that such strict colour maintenance could be a result of conserving an endogenous feeding rhythm similar to that observed in *Acartia tonsa* [59].

Cumulatively, our findings document a rare example of red structural colour in nature and is one of the few examples of multiple subwavelength nanostructures that combine to produce a single thin film capable of coherently scattering visible wavelengths of light. This novel colour production mechanism in arthropods illustrates a mechanism to produce and maintain brilliant red coloration with limited access to dietary pigments like carotenoids. Additionally, examining how nanolayers of air pockets incorporated into the exoskeleton could impact their vision could be an interesting avenue of research in the future

when studying copepods or other arthropods with similar bright red eyespots.

Data accessibility. The data and R code are provided in electronic supplementary material [60].

Authors' contributions. N.M.J.: conceptualization, data curation, formal analysis, investigation, methodology, writing—original draft, writing—review and editing; K.B.H.: conceptualization, data curation, formal analysis, investigation, methodology, writing—original draft, writing—review and editing; W.R.H.: funding acquisition, project administration, resources, supervision, writing—original draft, writing—review and editing; J.A.P.: data curation, formal analysis, writing—original draft, writing—review and editing; B.V.: data curation, formal analysis, writing—original draft, writing—review and editing; G.D.: data curation, formal analysis, writing—original draft, writing—review and editing; M.D.S.: funding acquisition, project administration, resources, writing—original draft, writing—review and editing; R.J.W.: methodology, writing—original draft, writing—review and editing; G.E.H.: funding acquisition, project administration, supervision, writing—original draft, writing—review and editing.

All authors gave final approval for publication and agreed to be held accountable for the work performed therein.

Conflict of interest declaration. The authors declare no competing interests.

Funding. This work was supported by National Science Foundation grant nos. IOS-1453784, OIA-1736150 and IOS-1754152, the Human Frontier Science Program RGP0047, FWO G007117 N and AFOSR grant no. FA-9550-18-1-0477 (M.D.S.).

Acknowledgements. We would like to thank Zhorro Nikolov for providing training and assistance with the Raman spectrometer. We thank the Auburn University Research Instrumentation Facility for access to microtoming and TEM equipment, and the Hill and Hood laboratory groups for edits on an early version of the manuscript. We also thank three anonymous reviewers for their comments throughout the review process.

References

1. Cuthill IC, Allen WL, Arbuckle K, Caspers B, Chaplin G, Hauber ME, Caro T. 2017 The biology of color. *Science* **357**, eaan0221. (doi:10.1126/science.aan0221)
2. Shawkey MD, D'Alba L. 2017 Interactions between colour-producing mechanisms and their effects on the integumentary colour palette. *Phil. Trans. R. Soc. B* **372**, 20160536. (doi:10.1098/rstb.2016.0536)
3. Justyn NM, Nallapaneni A, Parnell AJ, Karim A, Shawkey MD. 2022 A synergistic combination of structural and pigmentary colour produces non-spectral colour in the purple-breasted cotinga, *Cotinga cotinga* (Passeriformes: Cotingidae). *Biol. J. Linnean Soc.* **135**, 62–70. (doi:10.1093/biolinnean/blab144)
4. Elster A. 1896 Über einen Fundort von Diaptomus superbus, nebst einigen Bemerkungen über Farben der Copepoden. *Zool. Anz.* **96**, 245–251.
5. Weaver RJ, Cobine PA, Hill GE. 2018 On the bioconversion of dietary carotenoids to astaxanthin in the marine copepod, *Tigriopus californicus*. *J. Plank. Res.* **40**, 142–150. (doi:10.1093/plankt/fbx072)
6. Powlik JJ. 1996 Ecology of *Tigriopus californicus* (Copepoda, Harpacticoida) in Barkley Sound, British Columbia. Doctoral dissertation, University of British Columbia, Canada.
7. Fox DL. 1976 *Animal biochromes and structural colours*, 2nd edn. Berkeley, CA: University of California Press.
8. Balasubramaniam A. 2021 A bioinformatic analysis of the biosynthesis of carotenoids in the copepod *Tigriopus californicus*. Master's thesis, Wilfrid Laurier University, Canada.
9. Seligy VL. 1972 Ommochrome pigments of spiders. *Comp. Biochem. Physiol.* **41**, 699–709. (doi:10.1016/0300-9629(72)90448-3)
10. McGraw KJ. 2006 Pterins, porphyrins, and psittacofulvins. *Bird Color.: Mech. Meas.* **1**, 354. (doi:10.2307/j.ctv22jnscm.11)
11. Goldstein DH. 2005 Reflection properties of Scarabaeidae. *Polariz. Sci. Remote Sens. II* **5888**, 58880T. (doi:10.1117/12.618546)
12. Welch VL, Vigneron JP. 2007 Beyond butterflies—the diversity of biological photonic crystals. *Opt. Quant. Electron.* **39**, 295–303. (doi:10.1007/s11082-007-9094-4)
13. Seago AE, Brady P, Vigneron JP, Schultz TD. 2009 Gold bugs and beyond: a review of iridescence and structural colour mechanisms in beetles (Coleoptera). *J. R. Soc. Interface* **6**, S165–S184. (doi:10.1098/rsif.2008.0354.focus)
14. Fabricant SA, Kemp DJ, Krajíček J, Bosakova Z, Herberstein ME. 2013 Mechanisms of color production in a highly variable shield-back stinkbug, *Tectocoris diopthalmus* (Heteroptera: Scutelleridae), and why it matters. *PLoS ONE* **8**, e64082. (doi:10.1371/annotation/416a5460-d2e9-4d5b-87fa-c6c8659f002d)
15. Kariko S, Timonen JV, Weaver JC, Gur D, Marks C, Leiserowitz L, Li L. 2018 Structural origins of coloration in the spider *Phoroncidia rubroargentea* Berland, 1913 (Araneae: Theridiidae) from Madagascar. *J. R. Soc. Interface* **15**, 20170930. (doi:10.1098/rsif.2017.0930)
16. Gur D, Leshem B, Pierantoni M, Farstey V, Oron D, Weiner S, Addadi L. 2015 Structural basis for the brilliant colors of the sapphirinid copepods. *J. Am. Chem. Soc.* **137**, 8408–8411. (doi:10.1021/jacs.5b05289)
17. Gur D, Leshem B, Farstey V, Oron D, Addadi L, Weiner S. 2016 Light induced color change in the sapphirinid copepods: tunable photonic crystals. *Adv. Funct. Mater.* **26**, 1393–1399. (doi:10.1002/adfm.201504339)
18. Land MF. 1972 The physics and biology of animal reflectors. *Prog. Biophys. Mol. Biol.* **24**, 75–106. (doi:10.1016/0079-6107(72)90004-1)
19. Noyes JA, Vukusic P, Hooper IR. 2007 Experimental method for reliably establishing the refractive index of buprestid beetle exocuticle. *Opt. Express* **15**, 4351–4358. (doi:10.1364/OE.15.004351)
20. Magkiriadou S, Park JG, Kim YS, Manoharan VN. 2014 Absence of red structural color in photonic glasses, bird feathers, and certain beetles. *Phys. Rev. E* **90**, 062302. (doi:10.1103/PhysRevE.90.062302)
21. Hsiung BK, Justyn NM, Blackledge TA, Shawkey MD. 2017 Spiders have rich pigmentary and structural color palettes. *J. Exp. Biol.* **220**, 1975–1983. (doi:10.1242/jeb.156083)
22. Eliason CM, Maia R, Parra JL, Shawkey MD. 2020 Signal evolution and morphological complexity in hummingbirds (Aves: Trochilidae). *Evolution* **74**, 447–458. (doi:10.1111/evo.13893)
23. Eliason CM, Shawkey MD. 2010 Rapid, reversible response of iridescent feather color to ambient humidity. *Opt. Express* **18**, 21 284–21 292. (doi:10.1364/OE.18.021284)
24. Wilcox RE. 1964 Immersion liquids of relatively strong dispersion in the low refractive index range (1.46 to 1.52). *Am. Mineral.* **49**, 683–688.
25. Hsiung BK, Deheyn DD, Shawkey MD, Blackledge TA. 2015 Blue reflectance in tarantulas is evolutionarily conserved despite nanostructural diversity. *Sci. Adv.* **1**, e1500709. (doi:10.1126/sciadv.1500709)
26. Thomas DB, McGraw KJ, James HF, Madden O. 2014 Non-destructive descriptions of carotenoids in feathers using Raman spectroscopy. *Anal. Methods* **6**, 1301–1308. (doi:10.1039/C3AY41870G)
27. Heine KB, Justyn NM, Hill GE, Hood WR. 2021 Ultraviolet irradiation alters the density of inner mitochondrial membrane and proportion of inter-mitochondrial junctions in copepod myocytes. *Mitochondrion* **56**, 82–90. (doi:10.1016/j.mito.2020.11.001)
28. Hopkins CCE. 1978 The male genital system, and spermatophore production and function in *Euchaeta norvegica* Boeck (Copepoda: Calanoida). *J. Exp. Mar. Biol. Ecol.* **35**, 197–231. (doi:10.1016/0022-0981(78)90076-X)
29. Rueden CT, Schindelin J, Hiner MC, DeZonia BE, Walter AE, Arena ET, Eliceiri KW. 2017 ImageJ2: ImageJ for the next generation of scientific image data. *BMC Bioinf.* **18**, 529. (doi:10.1186/s12859-017-1934-z)
30. Leertouwer HL, Wilts BD, Stavenga DG. 2011 Refractive index and dispersion of butterfly chitin

and bird keratin measured by polarizing interference microscopy. *Opt. Express* **19**, 24 061–24 066. (doi:10.1364/OE.19.024061)

31. R Core Team. 2020 *R: a language and environment for statistical computing*. Vienna, Austria: R Foundation for Statistical Computing. See https://www.R-project.org/.
32. Maia R, Eliason CM, Bitton P-P, Doucet SM, Shawkey MD. 2013 pavo: an R package for the analysis, visualization and organization of spectral data. *Methods Ecol. Evol.* **10**, 906–913. (doi:10.1111/2041-210x.12069)
33. Arcangeli C, Cannistraro S. 2000 In situ Raman microspectroscopic identification and localization of carotenoids: approach to monitoring of UV-B irradiation stress on antarctic fungus. *Biopolym.: Orig. Res. Biomol.* **57**, 179–186. (doi:10.1002/(sici)1097-0282(2000)57:3<179::aid-bip6>3.0.co;2-4)
34. Focher B, Naggi A, Torri G, Cosani A, Terbojevich M. 1992 Structural differences between chitin polymorphs and their precipitates from solutions—evidence from CP-MAS ^{13}C-NMR, FT-IR and FT-Raman spectroscopy. *Carbohydr. Polym.* **17**, 97–102. (doi:10.1016/0144-8617(92)90101-U)
35. LaFountain AM, Prum RO, Frank HA. 2015 Diversity, physiology, and evolution of avian plumage carotenoids and the role of carotenoid–protein interactions in plumage color appearance. *Arch. Biochem. Biophys.* **572**, 201–212. (doi:10.1016/j.abb.2015.01.016)
36. Shawkey MD, Hauber ME, Estep LK, Hill GE. 2006 Evolutionary transitions and mechanisms of matte and iridescent plumage coloration in grackles and allies (Icteridae). *J. R. Soc. Interface* **3**, 777–786. (doi:10.1098/rsif.2006.0131)
37. Xiao M, Dhinojwala A, Shawkey M. 2014 Nanostructural basis of rainbow-like iridescence in common bronzewing *Phaps chalcoptera* feathers. *Opt. Express* **22**, 14 625–14 636. (doi:10.1364/OE.22.014625)
38. Ilagan RP, Christensen RL, Chapp TW, Gibson GN, Pascher T, Polivka T, Frank HA. 2005 Femtosecond time-resolved absorption spectroscopy of astaxanthin in solution and in α-crustacyanin. *J. Phys. Chem. A* **109**, 3120–3127. (doi:10.1021/jp0444161)
39. Elde AC, Pettersen R, Bruheim P, Järnegren J, Johnsen G. 2012 Pigmentation and spectral absorbance signatures in deep-water corals from the Trondheimsfjord, Norway. *Mar. Drugs* **10**, 1400–1411. (doi:10.3390/md10061400)
40. Lindon JC, Tranter GE, Koppenaal D. 2016 *Encyclopedia of spectroscopy and spectrometry*. Oxford, UK: Academic Press.
41. Heine KB, Powers MJ, Kallenberg C, Tucker VL, Hood WR. 2019 Ultraviolet irradiation increases size of the first clutch but decreases longevity in a marine copepod. *Ecol. Evol.* **9**, 9759–9767. (doi:10.1002/ece3.5510)
42. Hylander S, Grenvald JC, Kiorboe T. 2014 Fitness costs and benefits of ultraviolet radiation exposure in marine pelagic copepods. *Funct. Ecol.* **28**, 149–158. (doi:10.1111/1365-2435.12159)
43. Heine KB, Hood WR. 2020 Mitochondrial behaviour, morphology, and animal performance. *Biol. Rev.* **95**, 730–737. (doi:10.1111/brv.12584)
44. Shawkey MD, Hill GE, McGraw KJ, Hood WR, Huggins K. 2006 An experimental test of the contributions and condition dependence of microstructure and carotenoids in yellow plumage coloration. *Proc. R. Soc. B* **273**, 2985–2991. (doi:10.1098/rspb.2006.3675)
45. Bleiweiss R. 2005 Variation in ultraviolet reflectance by carotenoid-bearing feathers of tanagers (Thraupini: Emberizinae: Passeriformes). *Biol. J. Linn. Soc.* **84**, 243–257. (doi:10.1111/j.1095-8312.2005.00427.x)
46. Hill GE *et al.* 2019 Plumage redness signals mitochondrial function in the house finch. *Proc. R. Soc. B* **286**, 20191354. (doi:10.1098/rspb.2019.1354)
47. Powers MJ, Hill GE, Weaver RJ. 2020 An experimental test of mate choice for red carotenoid coloration in the marine copepod *Tigriopus californicus*. *Ethology* **126**, 344–352. (doi:10.1111/eth.12976)
48. Martin GG, Speekmann C, Beidler S. 2000 Photobehavior of the harpacticoid copepod *Tigriopus californicus* and the fine structure of its nauplius eye. *Invert. Biol.* **119**, 110–124. (doi:10.1111/j.1744-7410.2000.tb00179.x)
49. Werth AJ. 2012 Hydrodynamic and sensory factors governing response of copepods to simulated predation by Balaenid Whales. *Int. J. Ecol.* **2012**, 208913. (doi:10.1155/2012/208913)
50. Buskey EJ, Mann CG, Swift E. 1986 The shadow response of the estuarine copepod *Acartia tonsa* (Dana). *J. Exp. Mar. Biol. Ecol.* **103**, 65–75. (doi:10.1016/0022-0981(86)90132-2)
51. Buskey EJ, Hartline DK. 2003 High-speed video analysis of the escape responses of the copepod *Acartia tonsa* to shadows. *Biol. Bull.* **204**, 28–37. (doi:10.2307/1543493)
52. Cohen JH, Forward RB. 2002 Spectral sensitivity of vertically migrating marine copepods. *Biol. Bull.* **203**, 307–314. (doi:10.2307/1543573)
53. Cohen JH, Forward RB. 2005 Diel vertical migration of the marine copepod *Calanopia americana*. II. Proximate role of exogenous light cues and endogenous rhythms. *Mar. Biol.* **147**, 399–410. (doi:10.1007/s00227-005-1570-4)
54. Yoshida T, Toda T, Kuwahara V, Taguchi S, Othman BHR. 2004 Rapid response to changing light environments of the calanoid copepod *Calanus sinicus*. *Mar. Biol.* **145**, 505–513. (doi:10.1007/s00227-004-1343-5)
55. Stahl W, Heinrich U, Jungmann H, Sies H, Tronnier H. 2000 Carotenoids and carotenoids plus vitamin E protect against ultraviolet light-induced erythema in humans. *Am. J. Clin. Nutr.* **71**, 795–798. (doi:10.1093/ajcn/71.3.795)
56. Krinsky NI, Landrum JT, Bone RA. 2003 Biologic mechanisms of the protective role of lutein and zeaxanthin in the eye. *Ann. Rev. Nutr.* **23**, 171–201. (doi:10.1146/annurev.nutr.23.011702.073307)
57. Feldman T, Yakovleva M, Lindström M, Donner K, Ostrovsky M. 2010 Eye adaptation to different light environments in two populations of *Mysis relicta*: a comparative study of carotenoids and retinoids. *J. Crust. Biol.* **30**, 636–642. (doi:10.1651/09-3218.1)
58. Abdel-Aal ESM, Akhtar H, Zaheer K, Ali R. 2013 Dietary sources of lutein and zeaxanthin carotenoids and their role in eye health. *Nutrients* **5**, 1169–1185. (doi:10.3390/nu5041169)
59. Stearns DE. 1986 Copepod grazing behavior in simulated natural light and its relation to nocturnal feeding. *Mar. Ecol. Prog.* **30**, 65–76. (doi:10.3354/meps030065)
60. Justyn NM, Heine KB, Hood WR, Peteya JA, Vanthournout B, Debruyn G, Shawkey MD, Weaver RJ, Hill GE. 2022 A combination of red structural and pigmentary coloration in the eyespot of a copepod. FigShare. (doi:10.6084/m9.figshare.c.5978511)